Loss of vascular CD34 results in increased sensitivity to lung injury

Bernard C. Lo[1], Matthew J. Gold[1], Sebastian Scheer[1,2], Michael R. Hughes[1], Jessica Cait[1], Erin Debruin[1], Fanny S. F. Chu[3], David C. Walker[3], Hesham Soliman[1], Fabio M. Rossi[1], Marie-Renée Blanchet[4], Georgia Perona-Wright[5,6], Colby Zaph[1,2], Kelly M. McNagny[1]*

[1]The Biomedical Research Centre, University of British Columbia, Vancouver, British Columbia, V6T 1Z3, Canada

[2]Infection and Immunity Program, Biomedicine Discovery Institute, Department of Biochemistry and Molecular Biology, Monash University, Clayton, VIC, 3800, Australia

[3]Department of Pathology and Laboratory Medicine, University of British Columbia, Vancouver, British Columbia V6T 2B5, Canada

[4]Centre de recherche de l'Institut universitaire de cardiologie et de pneumologie de Québec, Université Laval, Québec G1V 4G5, Canada

[5]Department of Microbiology and Immunology, University of British Columbia, Vancouver, British Columbia V6T 1Z3, Canada

[6]Institute of Infection, Immunity & Inflammation, University of Glasgow, Glasgow, G12 8TA, United Kingdom

Keywords

CD34, Vascular Endothelia, Fibrosis, Lung Injury, Bleomycin, Influenza

*** Corresponding Author:**

Kelly M. McNagny

The Biomedical Research Centre

2222 Health Sciences Mall

Vancouver, BC V6T 1Z3, Canada

Tel: (604) 822-7824 Fax: (604) 604-822-7815

Email: kelly@brc.ubc.ca

Author Contributions: All authors contributed to experimental design and data analysis. B.C.L., M.J.G., S.S., M.R.H., J.C., E.D., F.S.F.C., H.S., and M.R.B. performed the experiments. B.C.L and K.M.M. wrote the manuscript with contributions from M.J.G., S.S., M.R.H., D.C.W., and G.P.W.

Sources of support: This work was supported by the AllerGen Networks Centres of Excellence (Strategic Initiative grant to K.M.M.) and Canadian Institutes of Health Research (MOP-137142 to K.M.M.). Funding for B.C.L. provided by a UBC 4YF; M.J.G. was supported by an AllerGen CAIDATI award.

Running title: CD34 maintains lung vascular integrity after injury

Word count: 4839

Abstract word count: 170

Abstract

Survival during lung injury requires a coordinated program of damage limitation and rapid repair. CD34 is a cell surface sialomucin expressed by epithelial, vascular and stromal cells that promotes cell adhesion, coordinates inflammatory cell recruitment, and drives angiogenesis. To test whether CD34 also orchestrates pulmonary damage and repair, we induced acute lung injury in wild type (WT) and *Cd34*$^{-/-}$ mice by bleomycin (BLM) administration. We found that *Cd34*$^{-/-}$ mice displayed severe weight loss and early mortality compared to WT controls. Despite equivalent early airway inflammation to WT mice, CD34-deficient animals developed interstitial edema and endothelial delamination, suggesting impaired endothelial function. Chimeric *Cd34*$^{-/-}$ mice reconstituted with WT hematopoietic cells exhibited early mortality compared to WT mice reconstituted with *Cd34*$^{-/-}$ cells, supporting an endothelial defect. CD34-deficient mice were also more sensitive to lung damage caused by influenza infection, showing greater weight loss and more extensive pulmonary remodeling. Together our data suggest that CD34 plays an essential role in maintaining vascular integrity in the lung in response to chemical- and infection-induced, tissue damage.

Introduction

Although the adult lung has a robust capacity to regenerate following injury, dysregulation of normal wound healing processes leads to fibrosis and loss of organ function. These observations have prompted extensive studies into identification of lung progenitor populations capable of facilitating lung repair (1, 2). The cell surface sialomucin CD34 is a widely used marker for the enrichment of primitive multipotent hematopoietic cells for bone marrow (BM) transplantation (3, 4). More recently, its utility as a marker for progenitor cells has been extended to non-hematopoietic subsets including muscle satellite cells (5), hair follicle stem cells (6), multipotent stromal cells (7, 8), bronchoalveolar stem cells (BASCs) (9, 10) and lung-resident endothelial progenitors (11). Since CD34 is highly expressed by multiple progenitor populations and downregulated in differentiated states, it has been hypothesized that CD34 may play a role in cycling of undifferentiated precursors (12), but functional studies instead suggest that CD34 is an important regulator of cell adhesion and chemotaxis. In lymphoid tissues, a distinct glycoform of CD34 is expressed by high endothelial venules (HEVs) and serves as a ligand for L-selectin on lymphocytes thereby mediating naïve cell recruitment to lymph nodes (13). While this suggests that CD34 can, in some cases, facilitate adhesion, this glycoform of CD34 is exquisitely specific to rare HEVs and, thus, is unlikely to promote adhesion in other tissues. CD34 is also expressed by a number of hematopoietic subsets including eosinophils (14, 15), mast cells (14, 16, 17), dendritic cell (DC) precursors (18), fibrocytes, and circulating endothelial progenitors (19, 20). Intriguingly, deletion of CD34 in mast cells results in homotypic aggregation suggesting an alternate role as a blocker of adhesion (17). We have also noted impaired chemokine-dependent migration of eosinophils arguing for a role in facilitating cell mobility and chemotaxis. Consistent with these observations, *Cd34*$^{-/-}$ mice are resistant to a variety of inflammatory diseases due to defective inflammatory cell recruitment to peripheral tissues (14, 15, 18, 21). While this suggests an important role for CD34 in inflammatory cell trafficking, its function on non-hematopoietic and structural cells during tissue remodeling remains unknown.

Because CD34 is expressed by cells thought to mediate lung regeneration (epithelia, endothelia and mesenchyme) we have now investigated its function in two

models of lung injury. Bleomycin (BLM) inhalation results in damage to pneumocytes and endothelia and is characterized by an inflammatory phase and vascular leak followed by the accumulation of extracellular matrix in the parenchyma resulting in abnormal alveolar architecture and compromised function (1, 22, 23). Based on the well-documented contribution of chronic inflammation to dysregulated tissue repair, we speculated that *Cd34*$^{-/-}$ mice would be protected from the development of fibrosis. Surprisingly, we find that *Cd34*$^{-/-}$ mice are extremely sensitive to BLM-induced damage and exhibit a higher incidence of morbidity and mortality than their WT counterparts. Ultrastructural analyses of BLM-treated *Cd34*$^{-/-}$ lungs reveal interstitial edema in the alveolar walls and delamination of endothelial cells from the basal lamina. Similar experiments with BM chimeric mice indicate that sensitivity to BLM is due to the selective loss of CD34 on non-hematopoietic cells. Moreover, *Cd34*$^{-/-}$ mice exhibited more pronounced evidence of epithelial remodeling in response to influenza infection. In aggregate, these studies argue that CD34 plays a protective role in maintaining vascular integrity and basal lamina adhesion and thereby facilitates tissue repair.

Materials and Methods

Mice

C57BL/6J (WT), *Cd34*$^{-/-}$, B6.SJL-Ptprc^{a}Pepc^{b}/BoyJ (CD45.1), and B6.129S4-Pdgfra$^{tm11(EGFP)Sor}$/J (PDGFRα ^{EGFP}) mice were maintained under specific pathogen-free conditions at the BRC. Chimeric mice were generated by transplanting 10^7 BM cells from mice expressing CD45.2 (WT or *Cd34*$^{-/-}$) or CD45.1 intravenously (i.v.) into lethally irradiated CD45.1 or CD45.2 recipients. BM reconstitution efficiency was assessed by congenic CD45 expression by peripheral blood leukocytes. All procedures were approved by the UBC Animal Care Committee.

Lung injury models

Mice were challenged with bleomycin (BLM) (PPC) endotracheally (e.t.) at a dose of 2.5 or 5.0 U/kg, or i.v. at a dose of 1.6 U/mouse. Static lung elastance was measured by performing volume-regulated perturbations on anesthetized and tracheotomized mice using a flexiVent apparatus (SCIREQ) (24). Mice were challenged intranasally with 2.90

x 10^3 EID_{50} of influenza A/strain PR8 (H1N1). Cytokines in bronchoalveolar lavage fluid (BALF) or lung homogenates were quantified using a V-plex multi-spot assay (Meso Scale Discoveries).

Histology and immunohistochemistry

Formalin-fixed and paraffin-embedded lungs were cut into 5-μm sections for Masson's trichrome or hematoxylin and eosin staining. For immunostaining, lung sections underwent antigen retrieval and were stained using antibodies against CD34 (RAM34) (eBiosciences), podocalyxin (AF1556) (R&D Systems), GFP (ab13970) (Abcam), vimentin (ab92547) (Abcam), surfactant protein C (AB3786) (Millipore), E-cadherin (36/E-cad) (BD), and keratin 5 (Poly9059) (Biolegend). Sections were then incubated with AlexaFluor-conjugated antibodies and mounted using Prolong Gold Antifade with DAPI (Life). Optical z-stack images were captured on a Leica SP5X confocal microscope and morphometric analysis was performed using ImageJ.

Assessment of pulmonary vascular leak

Vascular leak was evaluated by a modified Miles assay as described previously (25, 26). Mice were injected i.v. with 20 mg/kg Evans blue dye (EBD). After one hour, mice were anesthetized by intraperitoneal injection of avertin, followed by perfusion with 2 mM EDTA PBS. After excision, lungs were transferred to formamide for EBD extraction. The optical density of formamide was read at 620 nm and 740 nm on a spectrophotometer; the amount of dye per gram lung tissue was calculated using a lung specific correction factor (25, 26).

Transmission electron microscopy

Lungs were fixed in 2.5% glutaraldehyde in 0.1 M cacodylate buffer. Tissues were processed as described previously (27) and imaged using a FEI Tecnai 12 Transmission Electron Microscope.

Flow cytometry

BALF was collected by three tracheal instillations and aspirations of 1 mL PBS. Tissues

were digested with collagenase D (1.5 U/mL) and dispase II (2.4 U/mL) (Roche) for 30 minutes. Samples were then incubated with anti-CD16/32 to block nonspecific antibody binding. Fluorescence-conjugated antibodies to CD45 (I3/2), CD11c (N418), CD3e (145-2C11), CD8 (53.67), CD4 (GK1.5), B220 (RA3-6B2), Ly6B (7/4) (Abcam), SiglecF (E50-2440) (eBiosciences), CD34 (RAM34) (eBiosciences), CD31 (390) (eBiosciences), PDGFRα (APA5) (eBiosciences), Sca1 (D7) (eBiosciences), and EpCAM (G8.8) (eBiosciences) were used. For EdU uptake experiments, mice were given 1 mg EdU daily by intraperiotenal injections; EdU detection was performed using the Click-IT assay kit (Life). Data was acquired on a BD LSRII and analyzed with FlowJo Software. All antibodies were generated in-house (UBC AbLab) unless otherwise indicated.

Statistics

Survival data are presented as Kaplan-Meier curves and analyzed with a log rank test. Normality of the data was assessed using the Shapiro-Wilk test; Student's *t*-test or Mann-Whitney test were used to determine significance. Statistical analyses were performed using Prism 5.0.

Results

Early mortality but unaltered fibrosis in *Cd34*$^{-/-}$ mice following BLM challenge

To assess the role of CD34 in lung injury and fibrosis, *Cd34*$^{-/-}$ and WT mice were treated endotracheally with a single dose of BLM. Strikingly, after administration of 5.0 U/kg or 2.5 U/kg of BLM (e.t.), *Cd34*$^{-/-}$ mice showed a significant dose-dependent increased frequency of mortality compared with WT controls (Fig 1A & 1B). Nearly all mortality in *Cd34*$^{-/-}$ mice at the 2.5 U/kg BLM dose occurred prior to day 10. Since the onset of fibrosis in this model is known to occur at approximately two weeks following tracheal administration of BLM (23), these data suggest that early morbidity is associated with the acute exudative phase of the disease and independent of fibrosis. To further corroborate *Cd34*$^{-/-}$ mouse sensitivity to BLM in a systemic treatment regime, we assessed animal response following intravenous administration of 1.6 U/mouse BLM. Again, *Cd34*$^{-/-}$ mice experienced significantly greater weight loss than WT controls with nearly all *Cd34*$^{-}$

$^{-/-}$ animals reaching their humane endpoint by day 6 (Fig 1C). In summary, CD34 plays a protective role in bleomycin-induced lung injury prior to the development of fibrosis.

Although there was a clear increase in early mortality in *Cd34*$^{-/-}$ mice, sufficient numbers of these mice tolerated the lower dose of BLM to permit the evaluation of lung fibrosis 21 days after treatment. Quantitative analyses of Masson's trichrome stained lung sections revealed similar degrees of fibrotic remodeling in WT and *Cd34*$^{-/-}$ animals (Fig 1D & 1E). Moreover, static lung elastance was similar in BLM-treated WT and *Cd34*$^{-/-}$ animals suggesting that loss of CD34 does not alter this functional outcome of fibrosis (Fig 1F). To eliminate the possibility of a biased assessment of fibrosis selectively in mice that survived initial lung damage, we evaluated WT and *Cd34*$^{-/-}$ mice after endotracheal treatment with a lower BLM dose (1.25 U/kg) to ensure 100% survival by day 18 post-treatment. Again, no significant differences in fibrotic indices were observed between WT and *Cd34*$^{-/-}$ animals (Fig S1). We conclude that loss of CD34 exacerbates the early phase of BLM-induced injury but has no effect on the later fibrotic responses.

CD34 does not alter acute lung inflammation in response to BLM

Because we have previously observed attenuated allergic inflammatory responses in the lungs of *Cd34*$^{-/-}$ mice (14, 18), we evaluated whether the acute inflammation that occurs after BLM-treatment was altered by loss of CD34. Total $CD45^{+}$ leukocyte numbers in the BALF were similar in both WT and *Cd34*$^{-/-}$ mice three and six days after BLM-induced damage (Fig 2A). Differential analyses revealed equivalent frequencies of macrophage, neutrophil, and lymphocyte subsets (Fig 2B). The only significant alteration was a decrease in the frequency of infiltrating eosinophils (representing <3% of the infiltrate in WT mice and <1% in *Cd34*$^{-/-}$ mice) six days after BLM challenge (Fig 2B). This reflects a documented role of CD34 in recruitment of eosinophils to the lung (14, 28). We also observed similar levels of pro-inflammatory cytokines IL-1β, IL-6, CXCL1, and TNFα in damaged lung tissue of *Cd34*$^{-/-}$ and WT animals 6 days after damage (Fig 2C). In summary, because of the similar degree of inflammation, we conclude that differences in infiltrating inflammatory cells is unlikely to account for the increased mortality in BLM-treated *Cd34*$^{-/-}$ mice.

Interstital edema in BLM-treated *Cd34*$^{-/-}$ lung

Morbidity within the first week of BLM treatment can also be attributed to exacerbated exudative responses during acute lung injury; such pathological features include disruption of endothelial and epithelial barriers resulting in leakage of circulatory contents into the interstitium and edema (22, 29). We previously demonstrated increased vascular leak in lungs of *Cd34*$^{-/-}$ animals in a model of occupational asthma (18). To evaluate CD34 function in the maintenance of vascular integrity in response to acute lung injury, we assessed vascular leak in WT and *Cd34*$^{-/-}$ mice 6 days after bleomycin exposure using a modified Miles assay (25, 26). We found that *Cd34*$^{-/-}$ lung tissues displayed enhanced vascular leak as measured by Evans blue dye extracted from the lung interstitium (Fig 3A). Moreover, we observed a strong correlation between weight loss and severity of vascular leak (Fig 3B).

In our evaluation of histological sections of H&E-stained lung tissues 6 days after bleomycin treatment, we did not observe profound differences in pathology associated with acute respiratory distress (Fig S2). This prompted us to analyzed WT and *Cd34*$^{-/-}$ lungs at the ultrastructure level by TEM. Evaluation of PBS-treated WT and *Cd34*$^{-/-}$ lungs did not reveal differences in the structure or localization of interstitial collagen and elastin, alterations in capillary endothelial or type 1 epithelial tight junctions, or cell-basal lamina interactions (Fig S3). In contrast, six days after BLM challenge, we detected hypertrophy of type 1 pneumocytes in WT and *Cd34*$^{-/-}$ lung sections, which is indicative of injury (Fig 4A-F). Strikingly, BLM-treated *Cd34*$^{-/-}$ lung specimens exhibit extensive edema within the interstitium and delamination of the endothelia as evidenced by the exposed interstitial collagen and the disruption in the epithelial and capillary endothelial basal lamina interactions. Thus, the ultrastructure data suggests that CD34 plays a role in maintaining appropriate structural integrity of the alveolar wall in response to acute damage.

CD34 is expressed by endothelia and mesenchymal subsets, but not by epithelia in normal lung

While previous work has suggested that, in the lung, CD34 is expressed primarily by endothelial and mesenchymal cells, there are conflicting reports regarding the expression of CD34 on lung epithelial progenitors (9, 30, 31). To address this, we performed immunohistochemical analyses with antibodies against CD34 and used *Cd34*$^{-/-}$ lung samples as controls. CD34^{+} cells were detected in nearly all compartments except the large airway epithelia, with minimal background in knockout-control sections (Fig S4). From the analysis of confocal *z* stack images, CD34 is expressed by podocalyxin^{+} endothelia in addition to PDGFRα^{+} and vimentin^{+} fibrobroblast subsets (Fig 5A & 5B). Co-staining with antibodies against E-cadherin (E-cad) and surfactant protein C (SfpC) indicate that CD34 is not expressed by epithelia in the distal airways or the bronchoalveolar duct junctions (BADJs) where CD34-expressing epithelial progenitors were previously reported (Fig 5C) (9). This is consistent with flow cytometric data, which show that CD34^{+} cells co-stain with the endothelial specific antigen CD31 and the majority of PDGFRα^{+} fibroadipogenic progenitors (FAPs) enriched by Sca1^{+} selection. Moreover, we find a lack of CD34 expression in sorted EpCAM^{+} epithelial cells (Fig 5D).

Pulmonary fibroblasts represent a heterogeneous population; studies indicate that lung PDGFRα^{+} cells consist of desmin^{+} lipofibroblasts that support pneumocyte maintenance in alveolosphere cultures and proliferate in response to BLM treatment (32, 33). However, we saw equivalent expansion and proliferation of this fibroblast population in WT and *Cd34*$^{-/-}$ mice, analyzed six days following BLM damage (Fig 5E). We conclude that CD34 is not expressed by lung epithelial progenitors and, although it is expressed by fibroblasts, loss of CD34 has no effect on the proliferative response of these cells or their ability to produce matrix in late stage disease.

Early mortality in BLM-treated *Cd34*$^{-/-}$ mice is independent of its expression by hematopoietic cells

Previously, we observed increased vascular leakage in *Cd34*$^{-/-}$ mice during autoimmune arthritis (34) and, thus, we hypothesize that this vascular cell intrinsic function of CD34 could contribute to the early mortality phenotype observed in the current study. To conclusively exclude the possibility that this enhanced mortality reflects a defective

hematopoietic function for CD34, we generated BM chimeric mice with selective loss of CD34 in either the hematopoietic or non-hematopoietic compartments (Fig 6A & 6D). Following BLM challenge by endotracheal or intravenous treatment, lethally irradiated *Cd34*$^{-/-}$ mice transplanted with WT BM exhibited a significantly higher incidence of mortality and weight loss compared with the WT recipients (Fig 6B & 6C). Conversely, lethally irradiated WT CD45.1 animals transplanted with either *Cd34*$^{-/-}$ or WT BM and subsequently challenged with BLM displayed no significant differences in mortality rate or weight loss (Fig 6E & 6F). These data suggest that the selective loss of CD34 from non-hematopoietic tissues contributes to increased sensitivity to BLM challenge.

Loss of CD34 results in increased influenza infection-induced tissue remodeling

Next, we investigated whether CD34-deficiency altered responses to H1N1 influenza infection which induces extensive damage in the bronchioles and alveolar regions (1). Following infection, *Cd34*$^{-/-}$ mice displayed significantly greater weight loss than WT animals over the disease course (Fig 7A). Again, the overall inflammatory responses were similar in *Cd34*$^{-/-}$ and WT animals as the numbers of inflammatory infiltrates in the airways were comparable at days 7 and 12 post-infection (Fig 7B). Moreover, differential analyses indicate that myeloid, neutrophil, eosinophil, and lymphocyte subsets were unaltered due to loss of CD34 (Fig 7C). Interestingly, however, we found greater evidence of pathology in lung sections of *Cd34*$^{-/-}$ animals; this was assessed by the quantification of tissue area displaying abnormal alveolar architecture and high cellular density accompanied by loss of airway space (Fig 7D & 7E). Although we found that keratin 5 (Krt5) positive staining was restricted to the epithelial cells in the bronchioles of WT lung sections, Krt5-expressing clusters were more abundant, appearing in the peribronchial regions and in the distal airways of *Cd34*$^{-/-}$ lung tissues arguing for greater disease severity. In summary, we find that loss of CD34 results in more pronounced sensitivity to influenza-induced tissue injury as evidenced by unresolved tissue remodeling.

Discussion

Inflammatory mediators have a clear association with the development and progression

304 of lung fibrosis, particularly in cases arising from exposure to environmental irritants,
305 infection (35). Our previous work suggested a key role for CD34 in the recruitment of
306 inflammatory subsets and that *Cd34*$^{-/-}$ mice exhibit attenuated pathological features of
307 lung or intestinal inflammation (14, 15, 18, 21). However, the relevance of CD34 in
308 responses to lung injury, remodeling, and fibrosis, has not been examined. Given the
309 importance of CD34 in mast cell and eosinophil trafficking, we postulated a function in
310 fibrotic disease (12, 14, 17, 28). The accumulation of eosinophils and mast cells in the
311 lung has previously been associated with idiopathic pulmonary fibrosis (IPF). Elevated
312 eosinophils in the BALF is associated with poor prognosis (36); moreover, pathological
313 contributions of eosinophils to IPF have been attributed to the cytotoxic factors they
314 produce (37, 38), or the pro-fibrogenic factors that induce excessive remodeling (39-41).
315 Although we did observe a reduced frequency of eosinophils recruited to the lung in
316 *Cd34*$^{-/-}$ mice early after BLM treatment, this did not have a protective effect. Thus, in the
317 BLM model, eosinophils appear to be largely dispensable. Although eosinophilia and
318 Th2 cytokines have previously been reported to be promoters of BLM-induced fibrosis
319 (39, 40, 42), our findings are consistent with more recent studies demonstrating that the
320 fibrosis is primarily Th17 driven and independent of IL-13 signaling (43, 44).
321 Importantly, the pro-fibrotic effects of IL-17A have been highlighted in several disease-
322 associated contexts (45, 46).
323
324 Instead, loss of CD34 renders mice extremely sensitive to BLM-induced mortality with
325 animals displaying microstructural loss of endothelial cell integrity and interstitial edema.
326 Nearly all incidences of morbidity and mortality occur prior to the appearance of scarring
327 in the lungs and the late phase fibrosis and tissue remodeling is equivalent in WT and
328 *Cd34*$^{-/-}$ mice. Because the single-dose BLM treatment model is associated with a
329 transient and self-limiting fibrotic response we can not rule out a more subtle effect of
330 CD34 loss in more robust models of fibrosis (23). Nevertheless, our data suggest that
331 CD34 is dispensable for the debilitating production of matrix in response to lung injury
332 and that, instead, it plays a role during a transient window before the remodeling and
333 fibrotic response. This result was confirmed in a second, influenza-driven model of lung
334 injury where tissue remodeling is a prominent feature. Here too, CD34 appears to be

dispensable in the inflammatory response, but *Cd34*$^{-/-}$ mice displayed greater weight loss and their lungs displayed a more pronounced pathology, accompanied by the appearance of Krt5^{+} epithelial clusters in the bronchioles and in the distal airways. While Krt5^{+} epithelial progenitors are necessary for regeneration to restore gas exchange, their accumulation may be indicative of increased susceptibility to damage or unresolved tissue remodeling (47, 48).

Previously we have noted that loss of CD34 results in altered vascular integrity in a number of inflammatory settings including autoimmune arthritis (34), hypersensitivity pneumonitis (18), and tumour formation (49). Because we observed no major differences in the number of BALF infiltrates or levels of pro-inflammatory cytokines in *Cd34*$^{-/-}$ and WT animals our data suggest the exacerbated interstitial edema observed in *Cd34*$^{-/-}$ animals is a cell intrinsic defect of the endothelium. BM chimera experiments further support a non-hematopoietic origin of this phenotype as the mortality occurred in the absence of CD34 on hematopoietic cells. Vascular integrity can be modulated by changes in junctional proteins that alter cell-cell interactions and integrin-dependent cell-matrix interactions (50). Consistent with altered integrin dependent adhesion, but normal cell junctions, TEM evaluation of BLM-challenged *Cd34*$^{-/-}$ lungs reveals extensive interstitial edema yet the endothelial-endothelial junctional complexes remain intact. Thus, our data suggest that CD34 plays a role in maintaining the integrity of endothelial adhesion to the basal lamina.

In many ways, the decreased adhesion of *Cd34*$^{-/-}$ endothelia to basal lamina is counter-intuitive. Previously we have shown that CD34 and its close relative, podocalyxin, are heavily-glycosylated and negatively-charged sialomucins that provide an anti-adhesive quality to hematopoietic cells, developing endothelia and epithelial tumor cells (12, 17, 51-53). It is noteworthy, however, that we and others have found that the anti-adhesive podocalyxin and active integrin signaling cooperate to facilitate the establishment of distinct integrin-linked basolateral/matrix bound surfaces and integrin-free, podocalyxin-rich, non-adhesive apical domains (12, 25, 51, 54). Thus, loss of CD34 would weaken vessel integrity; an effect that we observe via TEM analyses of *Cd34*$^{-/-}$ endothelia after

BLM treatment. Integrin dependent adhesion is primarily regulated by changes in conformation (affinity) and activation dependent clustering (avidity) (55). Therefore we speculate that loss of CD34 prevents integrins from adopting an active conformation or limits the ability of integrins to effectively cluster at the basolateral domains and promote adhesion. Intriguingly, we have found that overexpression of CD34-type proteins in epithelial cell lines tends to facilitate segregation of apical and basolateral proteins and the establishment of these domains in cells undergoing primary adhesion (52). Moreover cells that lack these proteins exhibit a delay in the recruitment of integrins to basolateral domains. Thus, delamination of endothelia observed in the current study may reflect an impaired ability to properly localize active integrins to the basal lamina rather than a loss of integrin expression per se. Future studies aimed at detailed structure function analyses may provide mechanistic insights into the functional domains of CD34 required for modulating integrin sorting and function.

CD34 is a marker for progenitor subsets of non-hematopoietic cell types including muscle satellite cells, hair follicle stem cells, and mesenchymal progenitors (5-8). It has been postulated that its utility as an enrichment marker for undifferentiated cells could be extended to epithelial progenitors of the lung, namely bronchoalveolar stem cells (BASCs). These cells are proposed to exist at BADJs and have the potential to give rise to terminal epithelial cells of the bronchioles and distal airways (9). However, subsequent studies have reported that epithelial lineages lack CD34 expression (31, 56, 57). In the current manuscript we have used *Cd34*$^{-/-}$ mice, immunofluorescence staining of tissue sections, and spatial localization in lung to address this issue. By confocal analyses of naïve lung, we do not observe co-expression of CD34 and epithelial markers in BADJs. This is corroborated by the absence of CD34 expression by any EpCam^{+} epithelial fraction of lung-derived cells, a subpopulation believed to contain epithelial progenitor cells (56). Instead, CD34 is expressed by vascular endothelia and mesenchymal cells including vimentin^{+} fibroblasts and PDGFRα^{+} Sca1^{+} FAPs. FAPs were previously characterized as stromal cells that support skeletal muscle regeneration, and were more recently described in the lung as lipofibroblasts of the alveolar niche with an analogous function (32, 58). Previously we found that CD34 is dispensable for normal

function of FAPs (59). This is consistent with our observations that lung FAPs, in an acute response to BLM, expand in similar numbers and display similar rates of proliferation in WT and *Cd34*$^{-/-}$ animals. However, we may not formally rule out an additional role for CD34 in lung FAPs; the intimate association of these cells with the endothelium and their known role in tissue repair and matrix production highlights the importance of endothelial-FAP cell cross talk.

In summary, our data suggest that vascular CD34 serves a protective function during lung injury by enhancing the endothelial/matrix interactions and thereby preventing delamination and reducing permeability. Future structural and functional studies designed to identify the requisite domains of the molecule could offer insights into how this function could be modulated to treat pulmonary edema.

Acknowledgements

We thank BRC core members I. Barta (histology), T. Murakami (genotyping), W. Yuan (animal care), M. Williams (antibodies), R. Dhesi, and L. Rollins (media). Funding provided by the AllerGen Networks Centres of Excellence (Strategic Initiative grant to K.M.M.). B.C.L. is supported by a UBC Four Year Doctoral Fellowship; M.J.G. was supported by an AllerGen Canadian Allergy and Immune Diseaes Advanced Training Initiative award.

References

1. Hogan BL, Barkauskas CE, Chapman HA, Epstein JA, Jain R, Hsia CC, Niklason L, Calle E, Le A, Randell SH, Rock J, Snitow M, Krummel M, Stripp BR, Vu T, White ES, Whitsett JA, Morrisey EE. Repair and regeneration of the respiratory system: complexity, plasticity, and mechanisms of lung stem cell function. *Cell stem cell* 2014; 15: 123-138.
2. Wansleeben C, Barkauskas CE, Rock JR, Hogan BL. Stem cells of the adult lung: their development and role in homeostasis, regeneration, and disease. *Wiley interdisciplinary reviews Developmental biology* 2013; 2: 131-148.
3. Berenson RJ, Andrews RG, Bensinger WI, Kalamasz D, Knitter G, Buckner CD, Bernstein ID. Antigen CD34+ marrow cells engraft lethally irradiated baboons. *The Journal of clinical investigation* 1988; 81: 951-955.

4. Berenson RJ, Bensinger WI, Hill RS, Andrews RG, Garcia-Lopez J, Kalamasz DF, Still BJ, Spitzer G, Buckner CD, Bernstein ID, et al. Engraftment after infusion of CD34+ marrow cells in patients with breast cancer or neuroblastoma. *Blood* 1991; 77: 1717-1722.
5. Beauchamp JR, Heslop L, Yu DS, Tajbakhsh S, Kelly RG, Wernig A, Buckingham ME, Partridge TA, Zammit PS. Expression of CD34 and Myf5 defines the majority of quiescent adult skeletal muscle satellite cells. *The Journal of cell biology* 2000; 151: 1221-1234.
6. Trempus CS, Morris RJ, Bortner CD, Cotsarelis G, Faircloth RS, Reece JM, Tennant RW. Enrichment for living murine keratinocytes from the hair follicle bulge with the cell surface marker CD34. *The Journal of investigative dermatology* 2003; 120: 501-511.
7. Scherberich A, Di Maggio ND, McNagny KM. A familiar stranger: CD34 expression and putative functions in SVF cells of adipose tissue. *World journal of stem cells* 2013; 5: 1-8.
8. Traktuev DO, Merfeld-Clauss S, Li J, Kolonin M, Arap W, Pasqualini R, Johnstone BH, March KL. A population of multipotent CD34-positive adipose stromal cells share pericyte and mesenchymal surface markers, reside in a periendothelial location, and stabilize endothelial networks. *Circulation research* 2008; 102: 77-85.
9. Kim CF, Jackson EL, Woolfenden AE, Lawrence S, Babar I, Vogel S, Crowley D, Bronson RT, Jacks T. Identification of bronchioalveolar stem cells in normal lung and lung cancer. *Cell* 2005; 121: 823-835.
10. Yanagi S, Kishimoto H, Kawahara K, Sasaki T, Sasaki M, Nishio M, Yajima N, Hamada K, Horie Y, Kubo H, Whitsett JA, Mak TW, Nakano T, Nakazato M, Suzuki A. Pten controls lung morphogenesis, bronchioalveolar stem cells, and onset of lung adenocarcinomas in mice. *The Journal of clinical investigation* 2007; 117: 2929-2940.
11. Kawasaki T, Nishiwaki T, Sekine A, Nishimura R, Suda R, Urushibara T, Suzuki T, Takayanagi S, Terada J, Sakao S, Tatsumi K. Vascular Repair by Tissue-resident Endothelial Progenitor Cells in Endotoxin-induced Lung Injury. *American journal of respiratory cell and molecular biology* 2015.
12. Nielsen JS, McNagny KM. Novel functions of the CD34 family. *Journal of cell science* 2008; 121: 3683-3692.
13. Baumheter S, Singer MS, Henzel W, Hemmerich S, Renz M, Rosen SD, Lasky LA. Binding of L-selectin to the vascular sialomucin CD34. *Science* 1993; 262: 436-438.
14. Blanchet MR, Maltby S, Haddon DJ, Merkens H, Zbytnuik L, McNagny KM. CD34 facilitates the development of allergic asthma. *Blood* 2007; 110: 2005-2012.
15. Maltby S, Wohlfarth C, Gold M, Zbytnuik L, Hughes MR, McNagny KM. CD34 is required for infiltration of eosinophils into the colon and pathology associated with DSS-induced ulcerative colitis. *The American journal of pathology* 2010; 177: 1244-1254.
16. Drew E, Merkens H, Chelliah S, Doyonnas R, McNagny KM. CD34 is a specific marker of mature murine mast cells. *Experimental hematology* 2002; 30: 1211-1218.

17. Drew E, Merzaban JS, Seo W, Ziltener HJ, McNagny KM. CD34 and CD43 inhibit mast cell adhesion and are required for optimal mast cell reconstitution. *Immunity* 2005; 22: 43-57.
18. Blanchet MR, Bennett JL, Gold MJ, Levantini E, Tenen DG, Girard M, Cormier Y, McNagny KM. CD34 is required for dendritic cell trafficking and pathology in murine hypersensitivity pneumonitis. *American journal of respiratory and critical care medicine* 2011; 184: 687-698.
19. Asahara T, Murohara T, Sullivan A, Silver M, van der Zee R, Li T, Witzenbichler B, Schatteman G, Isner JM. Isolation of putative progenitor endothelial cells for angiogenesis. *Science* 1997; 275: 964-967.
20. Chamoto K, Gibney BC, Lee GS, Lin M, Collings-Simpson D, Voswinckel R, Konerding MA, Tsuda A, Mentzer SJ. CD34+ progenitor to endothelial cell transition in post-pneumonectomy angiogenesis. *American journal of respiratory cell and molecular biology* 2012; 46: 283-289.
21. Grassl GA, Faustmann M, Gill N, Zbytnuik L, Merkens H, So L, Rossi FM, McNagny KM, Finlay BB. CD34 mediates intestinal inflammation in Salmonella-infected mice. *Cellular microbiology* 2010; 12: 1562-1575.
22. Adamson IY, Bowden DH. The pathogenesis of bleomycin-induced pulmonary fibrosis in mice. *The American journal of pathology* 1974; 77: 185-197.
23. Moore BB, Hogaboam CM. Murine models of pulmonary fibrosis. *American journal of physiology Lung cellular and molecular physiology* 2008; 294: L152-160.
24. Vanoirbeek JA, Rinaldi M, De Vooght V, Haenen S, Bobic S, Gayan-Ramirez G, Hoet PH, Verbeken E, Decramer M, Nemery B, Janssens W. Noninvasive and invasive pulmonary function in mouse models of obstructive and restrictive respiratory diseases. *American journal of respiratory cell and molecular biology* 2010; 42: 96-104.
25. Debruin EJ, Hughes MR, Sina C, Liu A, Cait J, Jian Z, Lopez M, Lo B, Abraham T, McNagny KM. Podocalyxin regulates murine lung vascular permeability by altering endothelial cell adhesion. *PloS one* 2014; 9: e108881.
26. Moitra J, Sammani S, Garcia JG. Re-evaluation of Evans Blue dye as a marker of albumin clearance in murine models of acute lung injury. *Transl Res* 2007; 150: 253-265.
27. Yap DB, Walker DC, Prentice LM, McKinney S, Turashvili G, Mooslehner-Allen K, de Algara TR, Fee J, de Tassigny X, Colledge WH, Aparicio S. Mll5 is required for normal spermatogenesis. *PloS one* 2011; 6: e27127.
28. Suzuki A, Andrew DP, Gonzalo JA, Fukumoto M, Spellberg J, Hashiyama M, Takimoto H, Gerwin N, Webb I, Molineux G, Amakawa R, Tada Y, Wakeham A, Brown J, McNiece I, Ley K, Butcher EC, Suda T, Gutierrez-Ramos JC, Mak TW. CD34-deficient mice have reduced eosinophil accumulation after allergen exposure and show a novel crossreactive 90-kD protein. *Blood* 1996; 87: 3550-3562.
29. Adamson IY. Drug-induced pulmonary fibrosis. *Environmental health perspectives* 1984; 55: 25-36.
30. Chen H, Matsumoto K, Brockway BL, Rackley CR, Liang J, Lee JH, Jiang D, Noble PW, Randell SH, Kim CF, Stripp BR. Airway epithelial progenitors are region

specific and show differential responses to bleomycin-induced lung injury. *Stem cells* 2012; 30: 1948-1960.
31. Teisanu RM, Chen H, Matsumoto K, McQualter JL, Potts E, Foster WM, Bertoncello I, Stripp BR. Functional analysis of two distinct bronchiolar progenitors during lung injury and repair. *American journal of respiratory cell and molecular biology* 2011; 44: 794-803.
32. Barkauskas CE, Cronce MJ, Rackley CR, Bowie EJ, Keene DR, Stripp BR, Randell SH, Noble PW, Hogan BL. Type 2 alveolar cells are stem cells in adult lung. *The Journal of clinical investigation* 2013; 123: 3025-3036.
33. Rock JR, Barkauskas CE, Cronce MJ, Xue Y, Harris JR, Liang J, Noble PW, Hogan BL. Multiple stromal populations contribute to pulmonary fibrosis without evidence for epithelial to mesenchymal transition. *Proceedings of the National Academy of Sciences of the United States of America* 2011; 108: E1475-1483.
34. Blanchet MR, Gold M, Maltby S, Bennett J, Petri B, Kubes P, Lee DM, McNagny KM. Loss of CD34 leads to exacerbated autoimmune arthritis through increased vascular permeability. *Journal of immunology* 2010; 184: 1292-1299.
35. Wynn TA. Integrating mechanisms of pulmonary fibrosis. *The Journal of experimental medicine* 2011; 208: 1339-1350.
36. Schwartz DA, Van Fossen DS, Davis CS, Helmers RA, Dayton CS, Burmeister LF, Hunninghake GW. Determinants of progression in idiopathic pulmonary fibrosis. *American journal of respiratory and critical care medicine* 1994; 149: 444-449.
37. Hallgren R, Bjermer L, Lundgren R, Venge P. The eosinophil component of the alveolitis in idiopathic pulmonary fibrosis. Signs of eosinophil activation in the lung are related to impaired lung function. *The American review of respiratory disease* 1989; 139: 373-377.
38. Peterson MW, Monick M, Hunninghake GW. Prognostic role of eosinophils in pulmonary fibrosis. *Chest* 1987; 92: 51-56.
39. Gharaee-Kermani M, McGarry B, Lukacs N, Huffnagle G, Egan RW, Phan SH. The role of IL-5 in bleomycin-induced pulmonary fibrosis. *Journal of leukocyte biology* 1998; 64: 657-666.
40. Huaux F, Liu T, McGarry B, Ullenbruch M, Xing Z, Phan SH. Eosinophils and T Lymphocytes Possess Distinct Roles in Bleomycin-Induced Lung Injury and Fibrosis. *The Journal of Immunology* 2003; 171: 5470-5481.
41. Fichtner-Feigl S, Fuss IJ, Young CA, Watanabe T, Geissler EK, Schlitt HJ, Kitani A, Strober W. Induction of IL-13 Triggers TGF- 1-Dependent Tissue Fibrosis in Chronic 2,4,6-Trinitrobenzene Sulfonic Acid Colitis. *The Journal of Immunology* 2007; 178: 5859-5870.
42. Gharaee-Kermani M, Nozaki Y, Hatano K, Phan SH. Lung interleukin-4 gene expression in a murine model of bleomycin-induced pulmonary fibrosis. *Cytokine* 2001; 15: 138-147.
43. Sonnenberg GF, Nair MG, Kirn TJ, Zaph C, Fouser LA, Artis D. Pathological versus protective functions of IL-22 in airway inflammation are regulated by IL-17A. *J Exp Med* 2010; 207: 1293-1305.
44. Wilson MS, Madala SK, Ramalingam TR, Gochuico BR, Rosas IO, Cheever AW, Wynn TA. Bleomycin and IL-1beta-mediated pulmonary fibrosis is IL-17A dependent. *J Exp Med* 2010; 207: 535-552.

45. Wynn TA, Ramalingam TR. Mechanisms of fibrosis: therapeutic translation for fibrotic disease. *Nature medicine* 2012; 18: 1028-1040.
46. Lo BC, Gold MJ, Hughes MR, Antignano F, Valdez Y, Zaph C, Harder KH, McNagny KM. The orphan nuclear receptor RORa and group 3 innate lymphoid cells drive fibrosis in a mouse model of Crohn's disease. *Sci Immunol* 2016; 1: eaaf8864.
47. Kumar PA, Hu Y, Yamamoto Y, Hoe NB, Wei TS, Mu D, Sun Y, Joo LS, Dagher R, Zielonka EM, Wang de Y, Lim B, Chow VT, Crum CP, Xian W, McKeon F. Distal airway stem cells yield alveoli in vitro and during lung regeneration following H1N1 influenza infection. *Cell* 2011; 147: 525-538.
48. Zuo W, Zhang T, Wu DZ, Guan SP, Liew AA, Yamamoto Y, Wang X, Lim SJ, Vincent M, Lessard M, Crum CP, Xian W, McKeon F. p63(+)Krt5(+) distal airway stem cells are essential for lung regeneration. *Nature* 2015; 517: 616-620.
49. Maltby S, Freeman S, Gold MJ, Baker JH, Minchinton AI, Gold MR, Roskelley CD, McNagny KM. Opposing roles for CD34 in B16 melanoma tumor growth alter early stage vasculature and late stage immune cell infiltration. *PloS one* 2011; 6: e18160.
50. Goddard LM, Iruela-Arispe ML. Cellular and molecular regulation of vascular permeability. *Thrombosis and haemostasis* 2013; 109: 407-415.
51. Strilic B, Kucera T, Eglinger J, Hughes MR, McNagny KM, Tsukita S, Dejana E, Ferrara N, Lammert E. The molecular basis of vascular lumen formation in the developing mouse aorta. *Dev Cell* 2009; 17: 505-515.
52. Nielsen JS, Graves ML, Chelliah S, Vogl AW, Roskelley CD, McNagny KM. The CD34-related molecule podocalyxin is a potent inducer of microvillus formation. *PloS one* 2007; 2: e237.
53. Siemerink MJ, Hughes MR, Dallinga MG, Gora T, Cait J, Vogels IM, Yetin-Arik B, Van Noorden CJ, Klaassen I, McNagny KM, Schlingemann RO. CD34 Promotes Pathological Epi-Retinal Neovascularization in a Mouse Model of Oxygen-Induced Retinopathy. *PloS one* 2016; 11: e0157902.
54. Bryant DM, Roignot J, Datta A, Overeem AW, Kim M, Yu W, Peng X, Eastburn DJ, Ewald AJ, Werb Z, Mostov KE. A molecular switch for the orientation of epithelial cell polarization. *Dev Cell* 2014; 31: 171-187.
55. Carman CV, Springer TA. Integrin avidity regulation: are changes in affinity and conformation underemphasized? *Curr Opin Cell Biol* 2003; 15: 547-556.
56. McQualter JL, Yuen K, Williams B, Bertoncello I. Evidence of an epithelial stem/progenitor cell hierarchy in the adult mouse lung. *Proceedings of the National Academy of Sciences of the United States of America* 2010; 107: 1414-1419.
57. Teisanu RM, Lagasse E, Whitesides JF, Stripp BR. Prospective isolation of bronchiolar stem cells based upon immunophenotypic and autofluorescence characteristics. *Stem cells* 2009; 27: 612-622.
58. Joe AW, Yi L, Natarajan A, Le Grand F, So L, Wang J, Rudnicki MA, Rossi FM. Muscle injury activates resident fibro/adipogenic progenitors that facilitate myogenesis. *Nature cell biology* 2010; 12: 153-163.
59. Alfaro LA, Dick SA, Siegel AL, Anonuevo AS, McNagny KM, Megeney LA, Cornelison DD, Rossi FM. CD34 promotes satellite cell motility and entry into

614 proliferation to facilitate efficient skeletal muscle regeneration. *Stem cells* 2011;
615 29: 2030-2041.

616

617

Figure legends

Figure 1. BLM-treated *Cd34*$^{-/-}$ mice have increased incidence of mortality and weight loss but comparable fibrotic responses to WT mice. Mortality rates of WT and *Cd34*$^{-/-}$ mice challenged with a single dose of (A) 5.0 U/kg or (B) 2.5 U/kg BLM (e.t.). (A) $P < 0.001$ (n=3 or 5 per group). Data are from a single experiment. (B) $P < 0.02$ (n=8 or 9 per group). One of two independent experiments. Significance determined by log-rank test. (C) Weight loss of WT and *Cd34*$^{-/-}$ mice following treatment of 1.6 U/mouse BLM (i.v.). *, $P < 0.05$, Student's t-test (n=7-9 per group). Plots shown are representative of two independent experiments. (D) Representative Masson's trichrome-stained lung sections of WT and *Cd34*$^{-/-}$ mice 21 days after BLM treatment (2.5 U/kg). Scale bar = 200 μm. (E) Percent fibrotic area determined by quantifying area of fibrotic lesions normalized to total tissue area. ns, $P > 0.05$, Mann-Whitney test (n=10 or 5 per group) (F) Static elastance (Est) measurements of PBS and BLM-treated WT and *Cd34*$^{-/-}$ mice. *, $P < 0.05$, Mann-Whitney test (n=3-4 per PBS-treated group; n=4-5 per BLM-treated group).

Figure 2. BLM-induced acute lung inflammatory response is comparable in *Cd34*$^{-/-}$ and WT mice. (A) Enumeration of total CD45$^+$ hematopoietic cells in the BALF of mice treated with PBS (naïve) or BLM; mice were sacrificed and tissues harvested Day 3 or 6 post-treatment as indicated. (B) Differential analysis of infiltrating leukocyte subsets in the BALF by flow cytometry using the surface markers CD11c$^+$ (myeloid cells), Ly6B$^+$ (7/4) (neutrophils), CD11c$^-$ SiglecF$^+$ (eosinophils), CD3e$^+$ (T lymphocytes), and B220$^+$ (B lymphocytes). *, $P < 0.05$, Mann-Whitney test (n=3 per PBS-treated group; n=4-8 per BLM-treated group). Representative data from two independent experiments. (C) Quantification of IL-1β, IL-6, CXCL1, TNFα in BAL fluid and lung homogenates of naive mice or BLM-treated mice six days after injury (n=3-4 per PBS treated group; n=6-7 per BLM-treated group). Representative data from two independent experiments.

Figure 3. CD34-deficiency results in increased pulmonary vascular leak following BLM-induced injury. (A) Vascular permeability was assessed by a modified Mile's

assay six days after endotracheal BLM instillation. Data presented as μg EBD extracted per gram of lung tissue. *, $P = 0.014$, Student's t test (n=7 per group). (B) Pearson correlation of vascular leak and percent of initial body weight of *Cd34*$^{-/-}$ mice. $P = 0.19$, $r^2 = 0.315$. Representative data from two independent experiments.

Figure 4. Lung tissue ultrastructure reveals interstitial edema in BLM-challenged *Cd34*$^{-/-}$ mice. Transmission electron micrographs of (A-C) WT and (D-F) *Cd34*$^{-/-}$ lung 6 days after BLM-induced lung injury. Images shown are representative of at least 50 fields of view per sample. Lung specimens were sampled from four mice per genotype. AL, alveolus; EN, endothelial cell; F, fibroblast; T1, type 1 alevolar epithelial cell (AEC); T2, type 2 AEC; CL, capillary lumen; RBC, erythrocyte; COL, collagen; EL, elastin; INT, interstitium; E, edema.

Figure 5. CD34 is expressed by vascular endothelia and mesenchymal subsets but not epithelial cells in naïve mouse lung. (A-C) Confocal images from z stacks demonstrating CD34 co-expression with podocalyxin (Podxl)$^+$ endothelial cells and (A) PDGFRα$^+$ and (B) vimentin$^+$ fibroblasts. (C) E-cadherin (E-cad)$^+$ and surfactant protein C (Sfpc)$^+$ epithelial cells do not express CD34; inset displays higher magnification of a bronchoalveolar duct junction (BADJ). Scale bars = 50 μm and inset scale bar = 10 μm. Bv, blood vessel; br, bronchiole. (D) Histograms represent relative fluorescence intensity of a CD34 specific antibody to cellular subsets gated for CD31$^+$ endothelia, PDGFRα$^+$ Sca1$^+$ fibroadipogenic progenitors (FAPs), or EpCam$^+$ epithelial cells. Representative results from 2-3 naive animals. (E) Flow cytometric analysis of FAP percentages in the lineage negative (CD45$^-$, CD31$^-$) fraction of naïve mice (PBS) and in mice six days after BLM treatment (e.t.) (BLM). (F) Quantification of EdU uptake indicates lung FAP proliferation in response to BLM-induced injury. n.s., $P > 0.05$, Mann-Whitney test (n=2, 3 per PBS-treated group; n=5-6 per BLM-treated group).

Figure 6. Loss of CD34 in non-hematopoietic tissues results in increased sensitivity to BLM challenge. (A) BMT mice were generated by transplanting CD45.1 bone marrow cells into lethally irradiated WT or *Cd34*$^{-/-}$ host animals. (B) Survival curves of

mice treated with 2.5 U/kg BLM (e.t.). $P < 0.02$, log rank test (n=6-9 per group). (C) Weight loss of mice challenged with 1.6 U/mouse BLM (i.v.). *, $P < 0.05$, Mann-Whitney test (n=5-7 per group). (D) Lethally irradiated CD45.1 mice were reconstituted with bone marrow cells from WT or *Cd34*$^{-/-}$ mice. (E) Survival curves of mice treated with 2.5 U/kg BLM (e.t.) (n=5-6 per group). (F) Weight of BM chimeras challenged with 1.6 U/mouse BLM (i.v.) (n=6 per group).

Figure 7. *Cd34*$^{-/-}$ mice display increased weight loss and more pronounced tissue remodeling after influenza infection. (A) Weight loss of WT and *Cd34*$^{-/-}$ mice following intranasal infection with influenza A/PR8. *$P > 0.05$; * $P > 0.01$; ***$P > 0.001$, Student's t test (n=8 per group). (B-C) Enumeration of total CD45^{+} hematopoietic cells and leukocyte subsets in the BALF of influenza infected mice (n = 4 or 6 mice per group). (D) Quantification of damaged area normalized to total tissue area 12 days after influenza infection. *, $P > 0.05$, Student's t test (n=8 or 10 per group). (E) Representative hematoxylin and eosin stained lung sections of WT and *Cd34*$^{-/-}$ mice 12 days after infection. (F) Immunofluorescent images of lung sections as shown in (E) stained for podocalyxin (Podxl, red) and keratin 5 (Krt5, blue). Scale bar = 200 μm. Bv, blood vessel; br, bronchiole. Representative data from two independent experiments.

Figure 1.

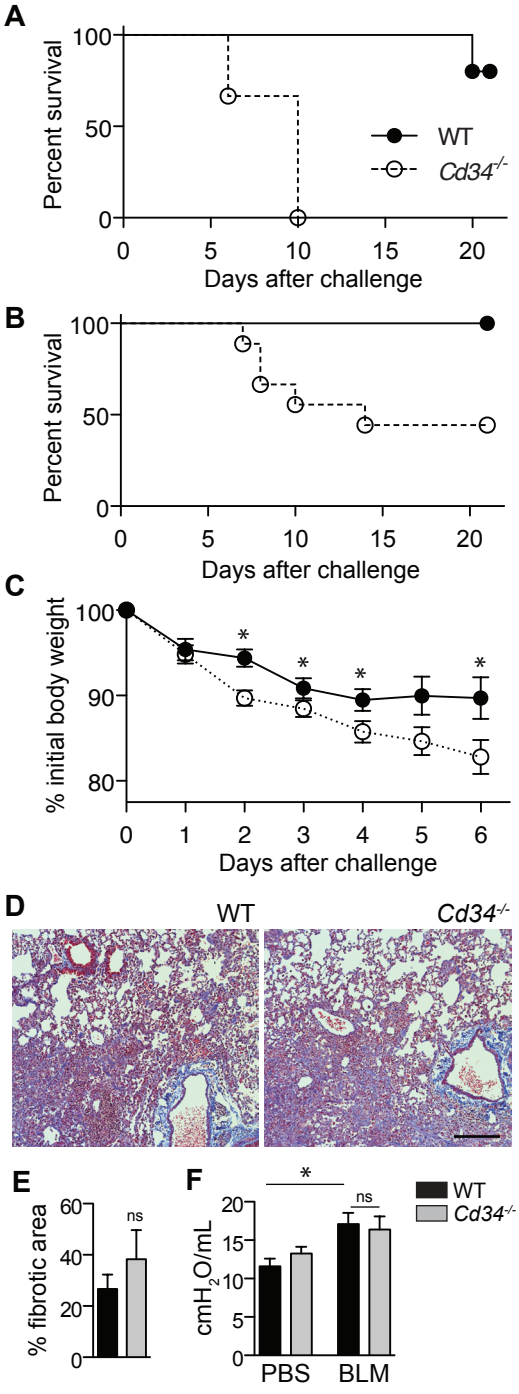
A
Percent survival
100
50
0
0
5
10
15
20
Days after challenge
WT
Cd34-/-
B
Percent survival
100
50
0
0
5
10
15
20
Days after challenge
C
% initial body weight
100
90
80
0
1
2
3
4
5
6
Days after challenge
*
D
WT
Cd34-/-
E
% fibrotic area
60
40
20
0
ns
F
cmH2O/mL
20
15
10
5
0
*
ns
PBS
BLM
WT
Cd34-/-

Figure 2.

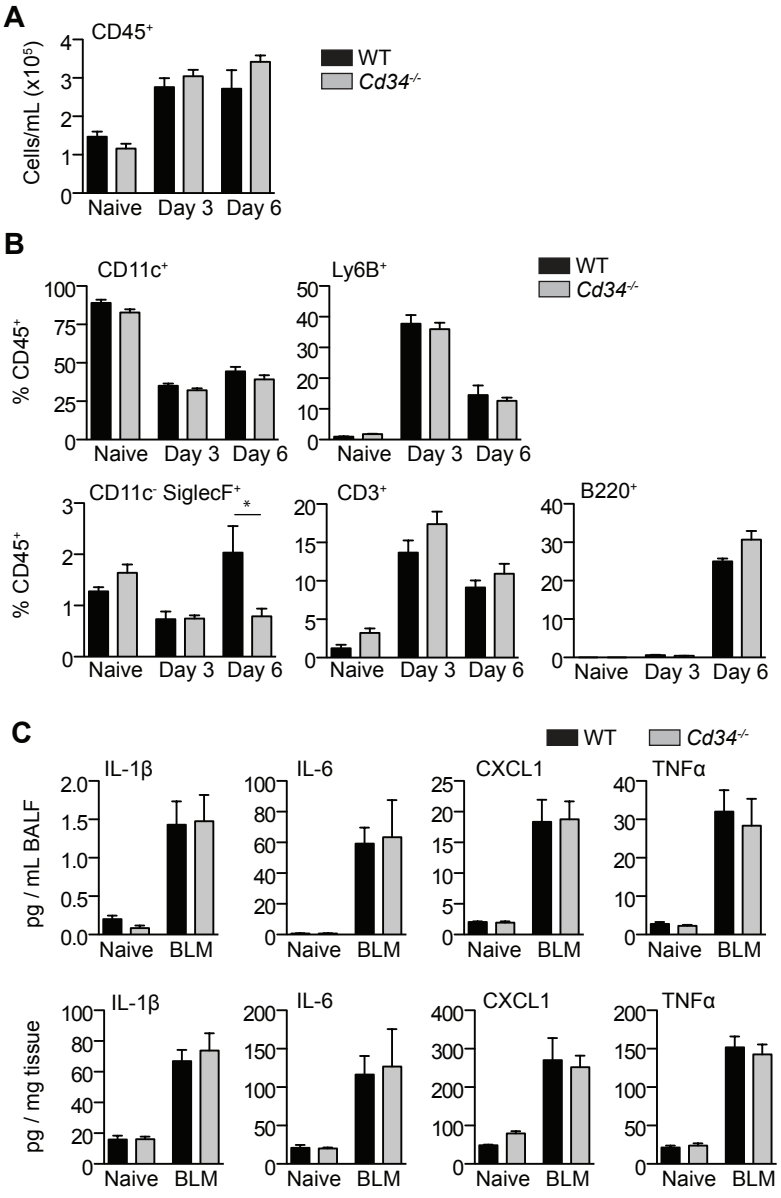
A
CD45+
Cells/mL (x10^5)
WT
Cd34-/-
Naive
Day 3
Day 6
B
CD11c+
Ly6B+
% CD45+
CD11c- SiglecF+
CD3+
B220+
*
C
IL-1β
IL-6
CXCL1
TNFα
pg / mL BALF
pg / mg tissue
BLM

Figure 3.

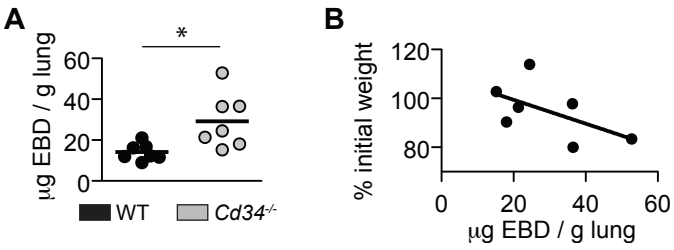
A
*
μg EBD / g lung
60
40
20
0
WT
Cd34-/-
B
% initial weight
120
100
80
0
20
40
60
μg EBD / g lung

Figure 4.

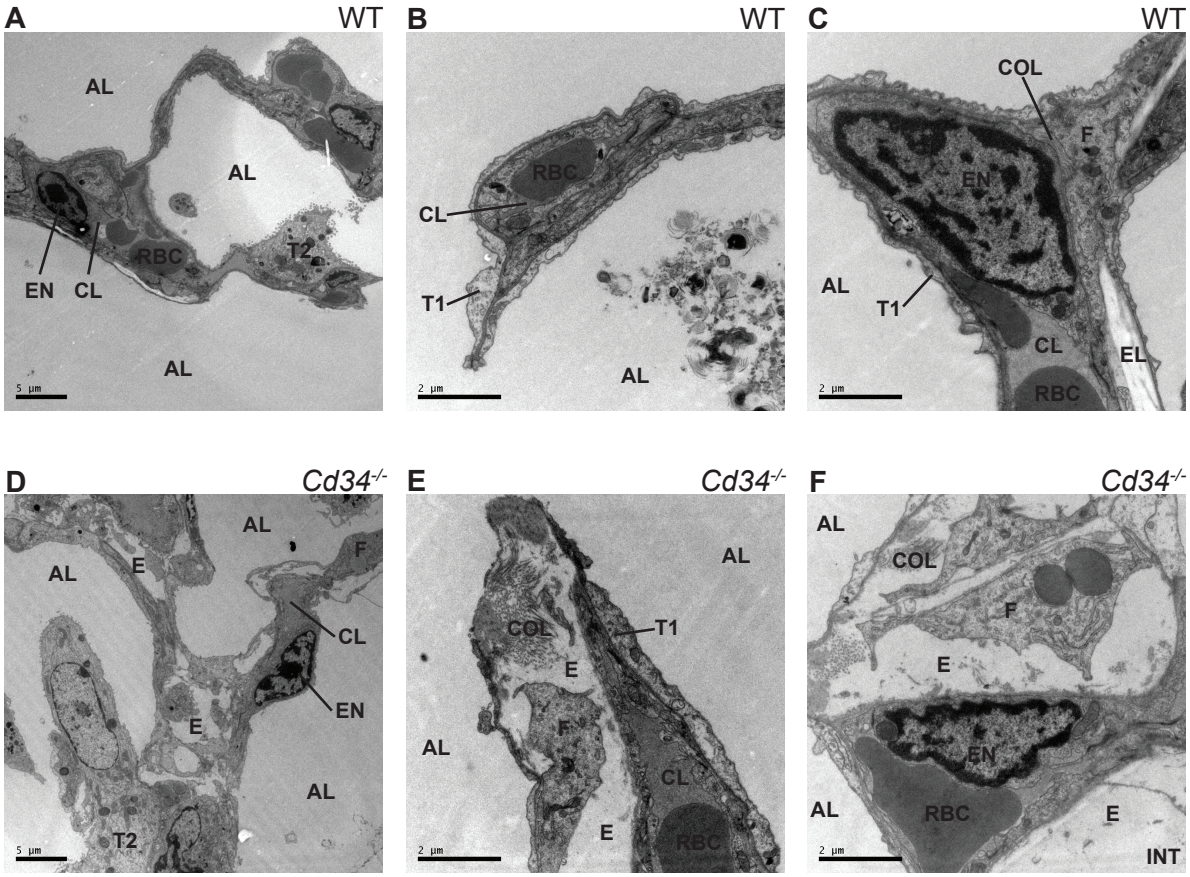
A
WT
AL
AL
RBC
T2
EN
CL
AL
5 µm
B
WT
RBC
CL
T1
AL
2 µm
C
WT
COL
F
EN
AL
T1
CL
EL
RBC
2 µm
D
Cd34-/-
AL
F
AL
E
CL
EN
E
AL
T2
5 µm
E
Cd34-/-
AL
COL
T1
E
F
AL
CL
E
RBC
2 µm
F
Cd34-/-
AL
COL
F
E
EN
AL
RBC
E
2 µm
INT

Figure 5.

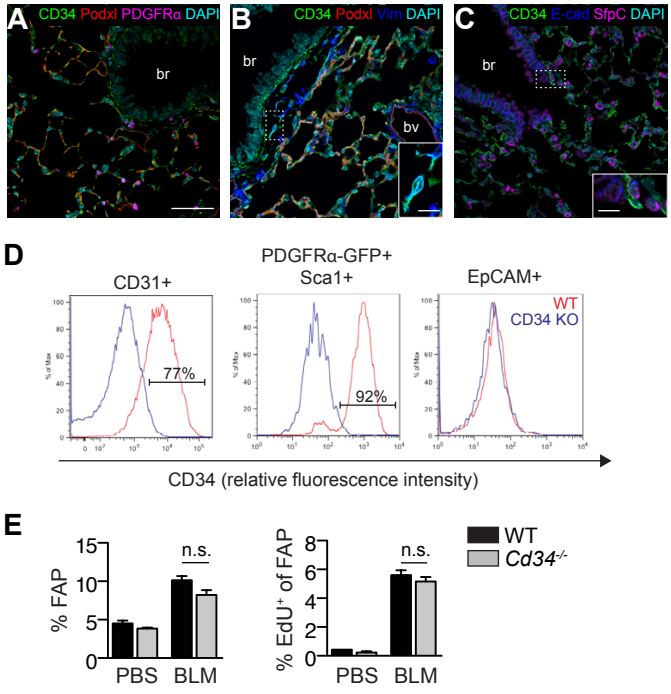
A
CD34 Podxl PDGFRα DAPI
br
B
CD34 Podxl Vim DAPI
br
bv
C
CD34 E-cad SfpC DAPI
br
D
CD31+
PDGFRα-GFP+
Sca1+
EpCAM+
WT
CD34 KO
77%
92%
CD34 (relative fluorescence intensity)
E
% FAP
15
10
5
0
n.s.
PBS
BLM
% EdU+ of FAP
8
6
4
2
0
n.s.
PBS
BLM
WT
Cd34-/-

Figure 6.

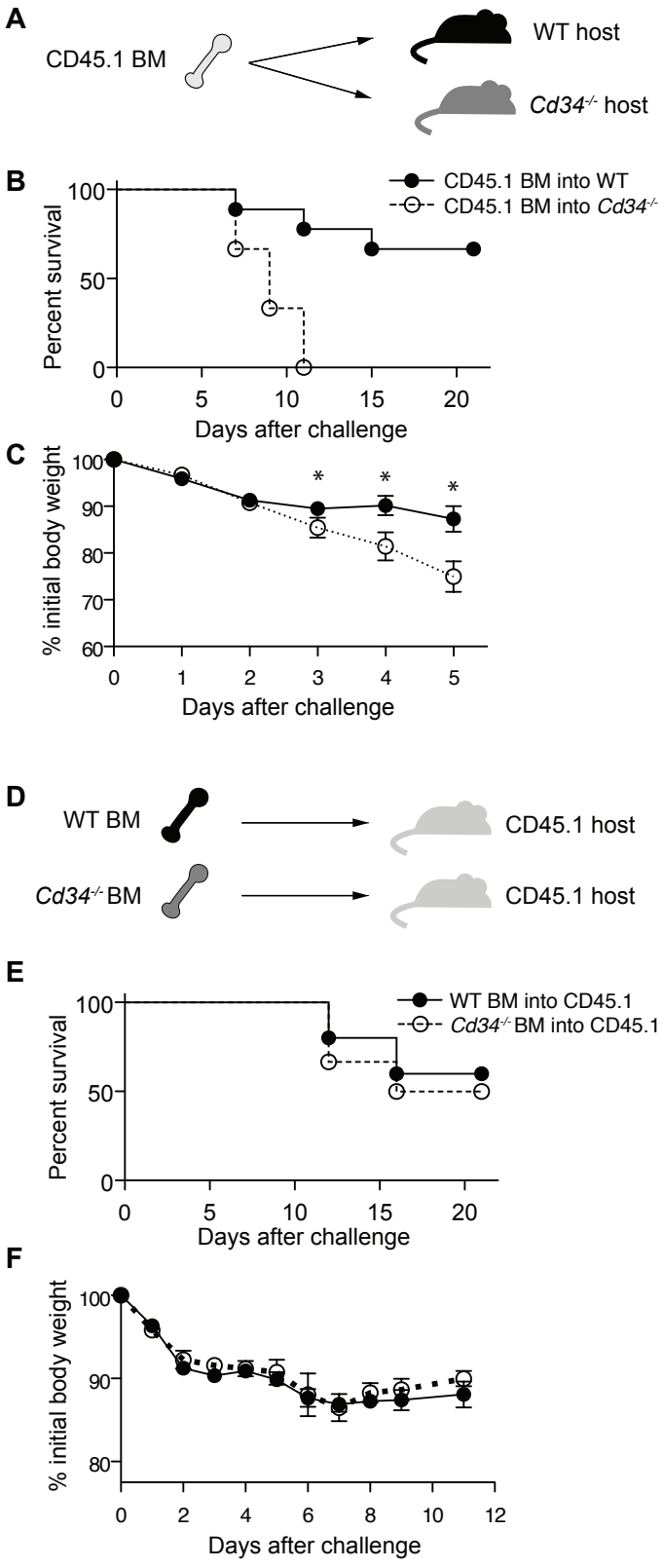
A
CD45.1 BM
WT host
Cd34-/- host
B
CD45.1 BM into WT
CD45.1 BM into Cd34-/-
Percent survival
100
50
0
0
5
10
15
20
Days after challenge
C
% initial body weight
100
90
80
70
60
0
1
2
3
4
5
Days after challenge
*
*
*
D
WT BM
Cd34-/- BM
CD45.1 host
CD45.1 host
E
WT BM into CD45.1
Cd34-/- BM into CD45.1
Percent survival
100
50
0
0
5
10
15
20
Days after challenge
F
% initial body weight
100
90
80
0
2
4
6
8
10
12
Days after challenge

Figure 7.

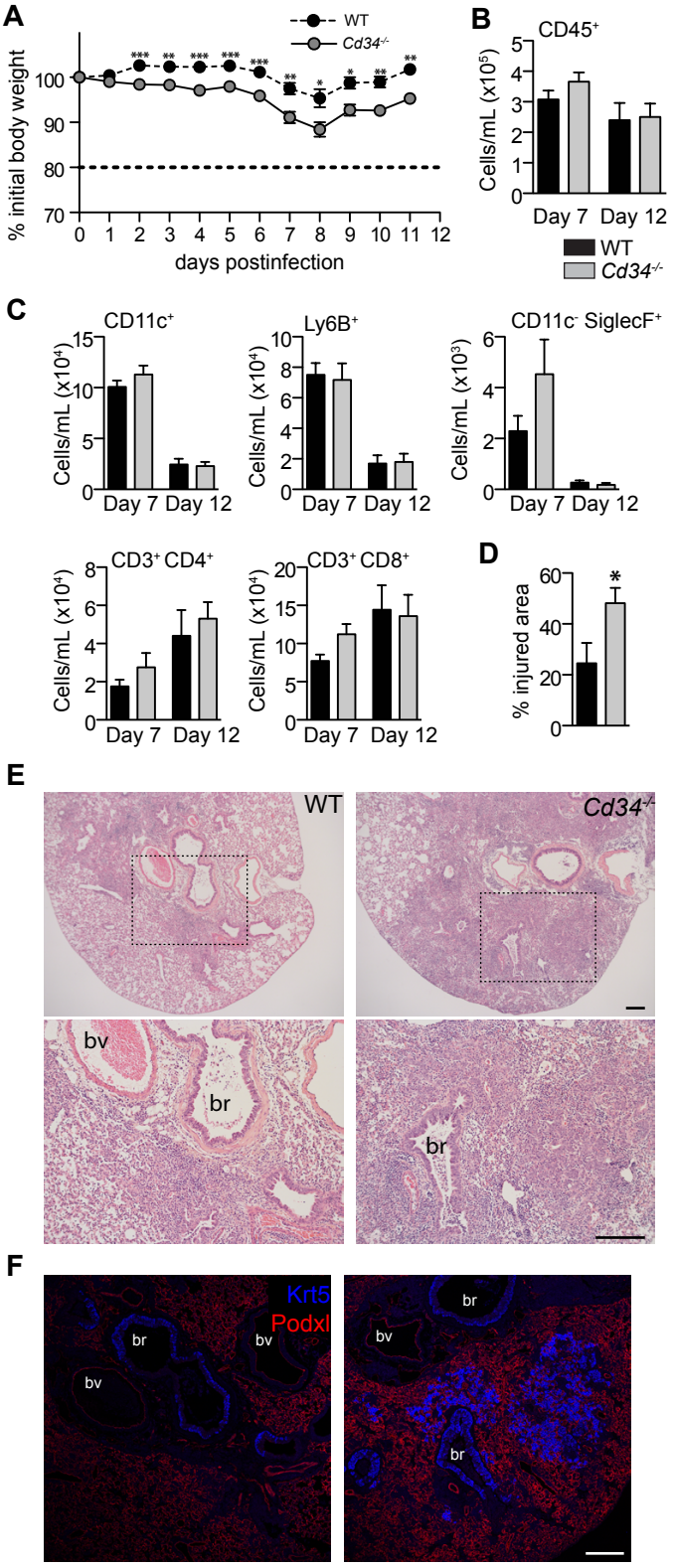
A
WT
Cd34-/-
% initial body weight
days postinfection
B
CD45+
Cells/mL (x10^5)
Day 7 Day 12
WT
Cd34-/-
C
CD11c+
Ly6B+
CD11c- SiglecF+
CD3+ CD4+
CD3+ CD8+
Cells/mL (x10^4)
Cells/mL (x10^3)
D
% injured area
E
WT
Cd34-/-
bv
br
F
Krt5
Podxl
br
bv